Comparison of simulation-based and measurement-based RF shimming for whole-body MRI at 7 Tesla

A. K. Bitz[1,2], I. Brote[1,2], S. Orzada[1,2], O. Kraff[1,2], S. Maderwald[1,2], H. H. Quick[3], K. Solbach[4], A. Bahr[5], H-P. Fautz[6], F. Schmitt[6], and M. E. Ladd[1,2]

[1]Erwin L. Hahn Institute for MRI, University Duisburg-Essen, Essen, Germany, [2]Department of Diagnostic and Interventional Radiology and Neuroradiology, University Hospital Essen, Essen, Germany, [3]Institute for Medical Physics, Friedrich-Alexander-University, Erlangen-Nuernberg, Germany, [4]High Frequency Technique, University Duisburg-Essen, Duisburg, Germany, [5]IMST GmbH, Kamp-Lintfort, Germany, [6]Siemens Healthcare Sector, Erlangen, Germany

Introduction: To investigate the clinical benefit of whole-body MRI at 7 Tesla with respect to diagnosis of pathological alterations, parallel transmit approaches such as Transmit SENSE [1, 2] or RF shimming [3, 4] have to be applied to mitigate effects caused by poor transmit field (B_1^+) homogeneity. In contrast to Transmit SENSE, the RF shimming approach transmits the same RF pulse envelope on each channel with individual amplitude and phase weightings optimized with respect to B_1^+ homogeneity. In one RF simulation study [5], such optimized weightings were derived for a ROI in the male pelvis from B_1^+ distributions in numerical body models. For in vivo examinations of the human prostate and heart, RF shimming parameters have also been derived from individually measured phase maps [6] and approximated relative B_1^+ maps [7]. Despite these already published case studies, it remains to be demonstrated that RF shimming is a useful concept to improve image quality in clinical examinations for various regions of interest in the thorax and abdomen of patients with varying physique. Therefore, the aim of this study was to compare the effectiveness of RF shimming procedures based on either RF simulations or on measured B_1^+ maps for different ROIs inside volunteers with different body masses.

Materials & Methods: Experiments were performed with an add-on system for RF shimming [8] including real-time SAR monitoring [9], which was integrated into a 7 T whole-body MR scanner (Magnetom 7 T, Siemens Healthcare, Erlangen, Germany), and a flexible 8-channel Tx/Rx body coil [10]. Simulated and measured B_1^+ distributions were imported into a graphical user interface which allows the selection of a ROI in the transverse plane for which the transmit field shall be optimized. Two shimming algorithms were applied: 1. a least-square optimizer which optimizes both amplitude and phase of the individual transmit channels, 2. an algorithm which adjusts only the phase of the channels and maintains equal amplitudes. For calculation of simulation-based RF shims, the complex B_1^+ distributions of the individual channels were computed (Microwave Studio, CST, Darmstadt, Germany) inside heterogeneous body models (male: 70 kg / 1.74 m, female: 58 kg / 1.6 m) [11]. In vivo B_1^+ mapping was performed during breath hold by utilization of a pre-saturation turboFLASH protocol provided by the vendor of the MR system. The sequence was adapted to the add-on RF shimming set-up by insertion of trigger pulses which drive the attenuators and phase shifters of the system in order to switch between single-element and common-mode excitation of the coil array when the saturation and read-out pulses are played out. Additionally, an ECG or pulse trigger was used for measuring B_1^+ maps in the heart. Shim effectiveness of the different approaches was compared by maps of the actual flip angle distribution and overall subjective image quality in the transverse plane for ROIs in the heart, liver, kidney, and prostate. Volunteers (heart = 6 male, 2 female; liver/kidney = 4 male, 4 female, prostate = 4) with a body height and body mass ranging from 1.65 m - 1.9 m and 65 kg - 100 kg were enrolled in the study.

Results: For certain body regions, shim weightings based on simulations offer acceptable B_1^+ homogeneity over multiple volunteers. Exemplarily, in Fig. 1 simulation-based and measured shims for cardiac imaging are shown; both are very similar. In 7 of 8 volunteers, the measured heart shim did not provide better B_1^+ characteristics than the simulation-based shim; only in one volunteer with a large heart was degraded B_1^+ homogeneity observed in the periphery of the heart. For certain ROIs, however, only measured shims achieve suitable transmit field distributions. Especially for the kidneys, whose shape and position can vary significantly within a group of volunteers, RF simulation results for a specific body model can lead to improper shim settings (Fig. 2a and b). This is especially the case if the numerical body model deviates considerably from the subject's body dimension and shape. In this case, subject-dependent shim modes (Fig. 2c and d) derived from measured B_1^+ maps of the individual transmit channels seem to be preferable. Fig. 2 reveals excellent image quality achieved in the large ROI covering both kidneys by applying the measured shim. As a last example, concerning liver imaging, experience has revealed that the second order clock-wise circularly polarized mode (CP^{2+}, 90° phase increment) is preferable, since it offers superior uniformity over the entire liver in subjects with varying physique (Fig. 3).

Conclusion: RF shimming was successfully applied to improve image quality in various ROIs located in the thorax and abdomen. Appropriate simulation-based shim modes, for which pre-calculation of SAR is possible, could be derived for the heart and liver which function in the majority of considered volunteers. If the numerical body model inadequately describes the subject's body, measured shims should be preferred to achieve higher image quality. This was found to be the case for renal imaging. Scaling the numerical body models according to the body size of the volunteers, however, might increase the application range of simulation-based shim modes.

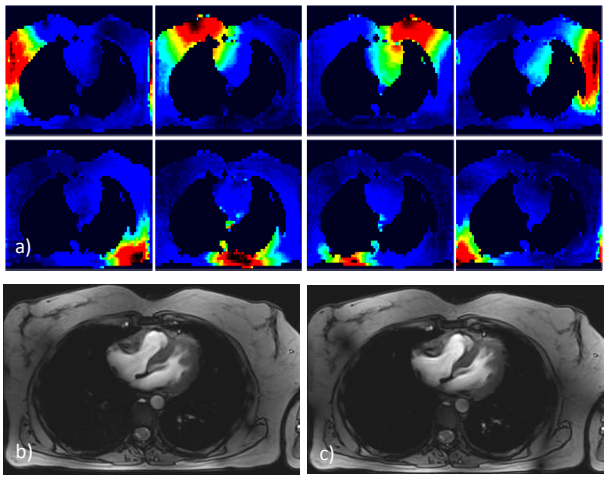

Fig. 1: RF shimming for cardiac MRI: female volunteer (1.65 m, 70 kg). a) Relative B_1^+ maps (pulse triggered) of individual transmit channels used for calculating the measured shim. Short-axis, cine FLASH, transverse plane: b) measured shim, c) simulation-based shim.

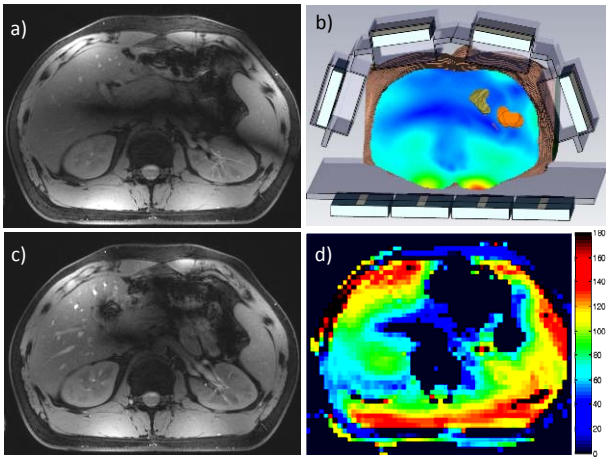

Fig. 2: RF shimming for MRI of the kidneys: male volunteer (1.9 m, 85 kg): a) Simulation-based shim, FLASH sequence, transverse plane, b) corresponding simulated B_1^+ distribution. c) Measured shim, FLASH sequence, transverse plane, d) measured absolute flip angle distribution.

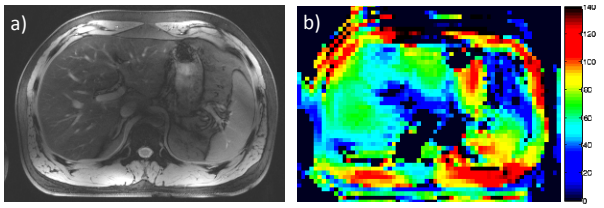

Fig. 3: RF shimming for MRI of the liver: male volunteer (1.86 m, 100 kg). a) FLASH with fat saturation, transverse plane, CP^{2+} mode; b) measured absolute flip angle distribution.

References: [1] Katscher et.al. MRM 2003; 49: 144-150. [2] Ullmann et.al. MRM 2005; 54: 994-1001; [3] Vaughan et.al. Proc. ISMRM 2005, 953; [4] Collins et. al. Proc. ISMRM 2005, 874; [5] v.d. Bergen et.al., Phys. Med. Biol. 52:5429–5441(2007); [6] Metzger et.al., MRM 59:396-409 (2008); [7] Snyder et.al., MRM 61:517-524 (2009); [8] Bitz et.al., Proc. ISMRM 17 (2009), 4767; [9] Brote et.al., Proc. ISMRM 17 (2009), 4788; [10] Orzada et.al. Proc. ISMRM 17 (2009), 2999; [11] Virtual Family Models, http://www.itis.ethz.ch/index/index_humanmodels.html.